Growth Kinetics of Polyethylene Single Crystals. I. Growth of (110) Faces of Crystals from Dilute Solutions in Xylene

M. Cooper and R. St. J. Manley*

The Pulp and Paper Research Institute of Canada, and the Department of Chemistry, McGill University, Montreal, Canada. *Received November 12, 1974*

ABSTRACT: The growth rates of polyethylene single crystals, as grown from xylene solutions, have been measured as a function of solution concentration, molecular weight of the polymer, and crystallization temperature. The following conclusions could be made: (1) the growth rate was found to be proportional to the concentration raised to a power less than unity; (2) the magnitude of the concentration exponent at a given crystallization temperature decreases as the molecular weight increases; (3) at a given molecular weight the exponent tends to increase as the crystallization temperature increases. These observations concerning the concentration dependence of the growth rate support the Sanchez–DiMarzio theory of self-nucleation (that is, cilia are able to perform the secondary nucleation required for continuing growth of a crystal). When considering the dependence of growth rate on molecular weight, the following trends were explained in terms of variation in the contributions of the cilia nucleation mechanism and the solution molecule nucleation mechanism to the overall nucleation process: (1) at a low, fixed concentration (0.001 wt %), under isothermal conditions, the growth rate continually increases with increasing molecular weight, suggesting that the cilia nucleation mechanism is dominant at low concentration; (2) at a "high," fixed concentration (0.1 wt %), at constant temperature, the growth rate initially increases with increasing molecular weight, but eventually passes through a broad maximum. This suggests that at this concentration most secondary nuclei are formed by molecules directly from solution; (3) thus on increasing the concentration from 0.001 to 0.1 wt % the profiles of the growth rate versus molecular weight curves change in character from that characteristic of a cilia nucleation mechanism to one characteristic of solution molecule nucleation. Using the Sanchez–DiMarzio estimates for the equilibrium dissolution temperature, and assuming that growth from solution is nucleation controlled, it was found that the apparent value of the surface free energy product, $\sigma\sigma_e$, increased with molecular weight. This tends to support the fractional stem rejection model (that is, that an end of a molecular chain smaller in length than the thickness of the crystal would be rejected by the crystal). The applicability of the Hoffman–Lauritzen regime theory to the dilute solution crystallization of polyethylene in the temperature range studied was discussed in relation to the theory of cilia nucleation. It appears that the assignment of a particular regime at any one temperature depends in part upon the molecular weight of the polymer.

During the past two decades much progress has been made in the understanding of the crystallization process in linear high polymers. The molecular chain folding that has been shown to be present in crystals formed under many conditions, both from the melt and in crystallization from solution, is now believed due to kinetic factors controlling the growth. The rate at which a crystal grows is of fundamental importance, for it is thought to determine, in part, the final structure of the crystal in terms of its fold length (long period), fold surface, and the general degree of crystallinity. The two major steps in the growth of a crystal are the formation of the primary nucleus and the secondary nucleation of each growth strip required for the continuing growth of the crystal. Several kinetic theories have attempted, with varying success, to account for the variation in the long period (l) with the undercooling and the unique values of l obtained under isothermal conditions.[1–5] Most of these theories deal with molecules of infinite molecular weight. The equilibrium dissolution temperature, and hence the undercooling, is known to vary with molecular weight and, in addition, the effects of the chain ends present in molecules of finite length should be considered.

A theory of polymer crystal growth recently proposed by Sanchez and Dimarzio includes predictions of the effects of molecular weight, concentration, and crystallization temperature on the growth rate of single crystals from dilute solution.[6,7] Data published to date are inadequate to test the theory, since most experiments have been performed with inadequately fractionated samples. It should be noted that measurement of the total rate of transformation, as by dilatometry, involves both nucleation and growth, and these processes must be separated to obtain information about the growth alone.

In the present paper, results are presented of growth rate studies of single crystals of linear polyethylene (as measured on the (110) faces) using several sharp molecular weight fractions under varying conditions of concentration and crystallization temperature (xylene was used as the solvent for all the results presented; the growth rates in other solvents will be discussed elsewhere). For an ideal test of the Sanchez–DiMarzio theory[1] (hereafter to be referred to as the S-D theory) monodisperse fractions of polymer should be used because molecular weight fractionation is thought to occur during the crystallization process. Such fractions are not available; however, the samples used in the present study are considered to be of sufficiently low polydispersity that fractionation will have little effect. Analysis of the results demonstrates that the S–D theory is consistent with the experimental data.

Materials

The characteristics of the six molecular weight fractions of linear polyethylene used throughout the investigation are listed in Table I.

The samples were prepared and characterized at the Centre de Recherches, Société Nationale des Pétroles d'Aquitaine, France. Six reference primary fractions were measured by light scattering experiments, allowing an analytical gel permeation chromatograph to be calibrated. The axial dispersion of the instrument was measured as a function of elution volume by reverse flow experiments.[8] The fractions were obtained by using the calibrated gpc at a preparative level[9] and were characterized by use of the following equations

$$\overline{M}_w = M_0 \exp(\sigma_m^2/2\pi)$$

$$\overline{M}_n = M_0 \exp(-\sigma_m^2/2)$$

$$P = \exp(\sigma_m^2)$$

Table I
Characteristics of the Polyethylene Fractions

$\bar{M}_w$	$\bar{M}_n$	P	T_s, °C
15,700	14,950	1.10	95.7
25,200	24,300	1.08	96.1
61,600	59,000	1.09	97.4
83,900	80,000	1.10	97.6
195,900	186,000	1.11	99.5
451,000	415,000	1.18	100.5

where σ represents the standard deviation, M_0 is the molecular weight at the apex of the peak on the gpc trace, and P is the polydispersity index. Such calculations were justified because the chromatograms were perfectly Gaussian in shape and the calibration curve was linear over the whole molecular weight range.

The xylene used was distilled prior to use. The growth experiments were conducted in oil baths adjusted to the desired temperatures (±0.02°).

Experimental Section

All polymer samples were weighed on a Cahn Electrobalance (±1 × 10^{-3} mg) and dissolved in xylene by refluxing under nitrogen. The solutions were crystallized at 85° (T_{c1}) and then cooled to room temperature. These crystal suspensions were used as stock samples in the crystallization kinetics experiments.

In order to facilitate the measurement of the crystals at intervals during their growth, the self-seeding method of Blundell, *et al.*,[10,11] was used throughout. Approximately 10 ml of the crystal suspension under study, contained in a test tube equipped with a ground glass stopper, was immersed in an oil bath held at 80°. The temperature was increased to some value T_s at a rate of 10°C min^{-1} and held at this temperature for 30 min. T_s was adjusted so as to leave crystal nuclei in suspension on which growth would begin immediately on transferring the sample tube to an oil bath set at the desired crystallization temperature (T_{c2}). The growth rate of the crystals was then uniform throughout any one preparation so that at any time all crystals had reached the same size. Measurement of about a dozen crystals at each sampling time during the growth indicated that the individual measurements were within 1% of the average.

The number of nuclei and hence the ultimate crystal size could be controlled by an appropriate choice of T_s. Values of T_s were chosen such that the growth rate was linear during the initial 1–3 μm of growth as measured from the center of a crystal to any (110) face. For any one molecular weight it was found that satisfactory results could be obtained when the value of T_s was within 0.2° of the most suitable temperature. T_s varied with molecular weight in the fashion shown in Table I when using crystal suspensions previously crystallized at 85°C.

On transferring the tube containing the nuclei suspension to a bath held at the desired crystallization temperature T_{c2}, approximately 2 min were required before isothermal conditions were attained. This was sufficiently rapid, in most cases, to ensure that almost no crystal growth occurred in the interim. This simple tube-transfer method proved inadequate when growth rates corresponding to higher undercoolings were studied. In these cases the hot seeded suspension was poured into a suitable volume of pure solvent held at T_{c2}. On using this method the shape and intercept of the crystal size *vs.* time curve indicated that the initial growth was linear and growth began within seconds of the moment of transfer.

The method of sampling the crystal population at any time was that of Blundell and Keller.[12] Periodically during growth a few drops were removed from the crystallizing solution and transferred to pure solvent at a lower temperature T_{c3}. The time at which the original isothermal growth had been interrupted was marked by a downward step in the crystal surface. This was due to the temperature change, the long period of a crystal being smaller when growth occurs at a lower temperature. On allowing the crystals to complete growth they could then be spotted onto grids, shadowed, and observed in the electron microscope. The linear crystal dimensions as measured from the center of a crystal up to the step on a (110) growth face were plotted as a function of time of the corresponding crystallization. Linear growth with time, during the initial stages of growth, was observed in all cases. The slope of the plot of crystal size *vs.* time gave the growth rate which was studied under varying conditions of temperature, concentration, and molecular weight.

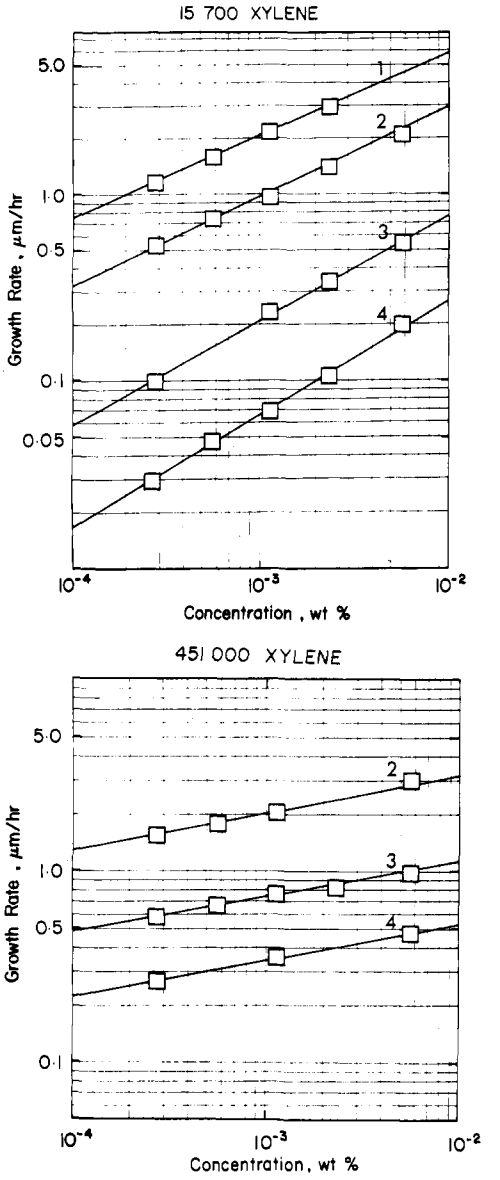

Figure 1. Logarithmic plots of the growth rate (μm/hr) of the (110) faces as a function of concentration (wt %) for two of the polyethylene fractions studied: top, $\bar{M}_w$ = 15,700; bottom, $\bar{M}_w$ = 451,000. The crystallization temperatures (T_c) are as follows (curve no., T_c (deg C)): 1, 86.60; 2, 87.90; 3, 89.90; 4, 90.70.

The choice of T_{c3} was mainly dictated by the molecular weight under study. On using the sample $\bar{M}_w$ = 15,700, it was found that simple monolayer growth would occur below 78°. This permitted large, clear steps to be formed on transferring from T_{c2} to T_{c3} because of the large difference in long period characteristic of the two temperatures. As progressively higher molecular weights were used, the lowest temperature at which simple monolayers would continue to grow was found to increase. The sample of $\bar{M}_w$ = 451,000 required a minimum T_{c3} of 87°; at temperatures below this, spiralled terrace growth covered the step which was to be used for measurements.

On occasion, for the samples of $\bar{M}_w$ = 195,900 and $\bar{M}_w$ = 451,000, it was found to be more convenient to use a T_{c3} of higher temperature than T_{c2}, the step on the crystal surface then being upward when viewed from the center of the crystal.

For convenience the one value of 82° for T_{c3} was used throughout when studying the lower four molecular weight fractions.

Studies were conducted only at those temperatures at which comparative measurements could be made encompassing the whole range of polymer molecular weight available.

Table II
Values of the Growth Rate of (110) Faces as a Function of Concentration and Temperature for Each of the Polyethylene Fractions Studied, Together with the Concentration Exponent as a Function of Crystallization Temperature[a]

Cryst temp, deg C	Concn, wt %	M_w = 15,700		M_w = 25,200		M_w = 61,600		M_w = 83,900		M_w = 195,900		M_w = 451,000	
		G	α	G	α	G	α	G	α	G	α	G	α
86.60	0.1	5.75		6.75		8.50		8.25		7.00			
	0.01	2.05	0.438	2.85	0.385	3.80	0.350	3.90	0.320	4.70	0.205		
	0.001	0.75		1.15		1.70		1.90		2.75			
87.90	0.1	3.00		4.00		5.00		4.90		4.10		3.2	
	0.01	1.00	0.495	1.55	0.410	2.15	0.370	1.95	0.370	2.40	0.240	2.0	0.195
	0.001	0.31		0.60		0.90		0.90		1.37		1.3	
89.80	0.1	0.75		1.1		1.50		1.60		1.35		1.15	
	0.01	0.23	0.560	0.42	0.419	0.65	0.390	0.67	0.380	0.72	0.265	0.74	0.189
	0.001	0.057		0.16		0.25		0.28		0.40		0.48	
90.70	0.1	0.26		0.41		0.83		0.83		0.67		0.53	
	0.01	0.06	0.595	0.16	0.457	0.32	0.403	0.33	0.385	0.34	0.265	0.34	0.190
	0.001	0.017		0.05		0.13		0.14		0.20		0.22	

[a] The solvent used was xylene. G = growth rate (μm/hr); α = concentration exponent.

Table III
Growth Rate Data for the (110) Faces of Polyethylene Single Crystals from Xylene Solution

		G (μm/hr) at M_w					
$T \pm 0.02°$	Concn, wt %	15,700	25,200	61,600	83,900	195,900	451,000
86.60	0.0029	1.15	1.75	2.40	2.65	3.30	
	0.0058	1.55	2.32	3.07	3.16	4.05	
	0.0116	2.21	2.90	4.05	4.13	4.80	
	0.023	2.90	4.02	5.20	4.90	5.50	
	0.058		5.55	7.00		7.00	
87.90	0.0029	0.53	0.90	1.35	1.23	1.80	1.53
	0.0058	0.76	1.21	1.76	1.58	2.00	
	0.0116	0.95	1.53	2.31	2.05	2.10	1.75
	0.023	1.48	2.27	3.00	2.75	3.10	2.00
	0.058	2.04	3.20	4.08	4.00	3.40	3.00
89.80	0.0029	0.11	0.24	0.39	0.44	0.53	0.58
	0.0058		0.33	0.53	0.53	0.60	0.65
	0.0116	0.24	0.44	0.65	0.70	0.75	0.78
	0.0155			0.75			
	0.023	0.34	0.60	0.88	0.88	0.85	0.83
	0.058	0.54	0.85	1.20	1.40	1.10	1.00
90.70	0.0029	0.03	0.09	0.22	0.21	0.28	0.26
	0.0058	0.05	0.12	0.25	0.28	0.33	
	0.0116	0.07	0.17	0.34	0.33	0.40	0.35
	0.023	0.11	0.22	0.46	0.45	0.45	
	0.058	0.21	0.33	0.67	0.68	0.60	0.49

[a] T_c = crystallization temperature; concn = concentration of the solution; G = growth rate; M_w = weight average molecular weight of the polyethylene sample. G corresponds to half the perpendicular distance measured between opposing (110) faces in the crystal.

In many cases duplicate experiments were made and gave results within the estimated precision (±1%).

The measurement of the growth of any one crystal could be made within 1% from both electron micrographs and a calibrated fluorescent screen within the microscope. Another error was encountered in the stability of the oil baths used for controlling the temperature of crystallization. The desired temperature could be held within ±0.02°. The variation of growth with temperature is largest at the highest growth rates. A growth rate of 8 μm hr^{-1} (among the highest of the growth rates reported here) should be read as 8 ± 0.05 μm hr^{-1} when taking into consideration the fluctuations of the bath. This is less than ±1%. On considering other errors such as those encountered in preparing the solution, any evaporation of solvent that could occur, and the precision with which the time of sampling could be measured, the growth rates appearing in the tables to follow may be considered valid to within about ±2%.

Results

The concentration dependence of the growth of a crystal may be described by the relation

$$G \propto C^{\alpha} \quad (1)$$

where G is the growth rate, C is the concentration, and α is a constant, termed the concentration exponent. In Figure 1 illustrative logarithmic plots of growth rate against concentration are presented for two of the fractions studied. In Table II, the results obtained for the growth rates of the (110) faces in single crystals from the six molecular weight fractions, under varying conditions of crystallization temperature and solution concentration, are shown together with the values for α obtained from the slopes of the

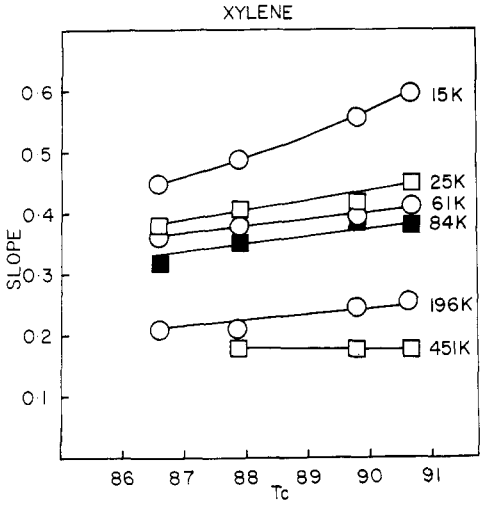

Figure 2. The variation of the concentration exponent (slope) with the temperature of crystallization for the molecular fractions studied. The molecular weights are indicated, *e.g.*, $15K \equiv \bar{M}_w$ 15,700.

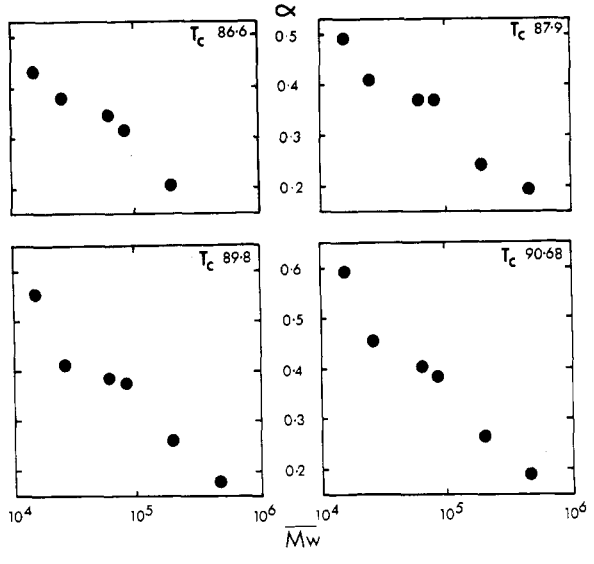

Figure 3. The concentration exponent α *vs.* molecular weight for the four crystallization temperatures T_c (deg C).

curves. The growth rates in the table are those corresponding to concentrations of 0.1, 0.01, and 0.001 wt % as extrapolated or interpolated from the straight lines drawn through the experimental points. In Table III all the original experimental points are listed.

Discussion

Concentration Dependence of Growth Rate. In earlier studies of the growth rates of polyethylene single crystals from dilute xylene solutions,[12-14] the growth was found to be proportional to the concentration raised to a power less than unity. These data were obtained using unfractionated polymer samples, for which the polydispersity was unknown,[12,13] and poorly fractionated polymer.[14] Keller and Pedemonte[14] reported that the concentration exponent (α) increased with the temperature of crystallization for all samples studied. As indicated above, the samples used by Keller were either unfractionated or of relatively high polydispersity and, since it has been anticipated that fractionation would influence the magnitude of α and its variation with molecular weight and crystallization temperature,[7,15]

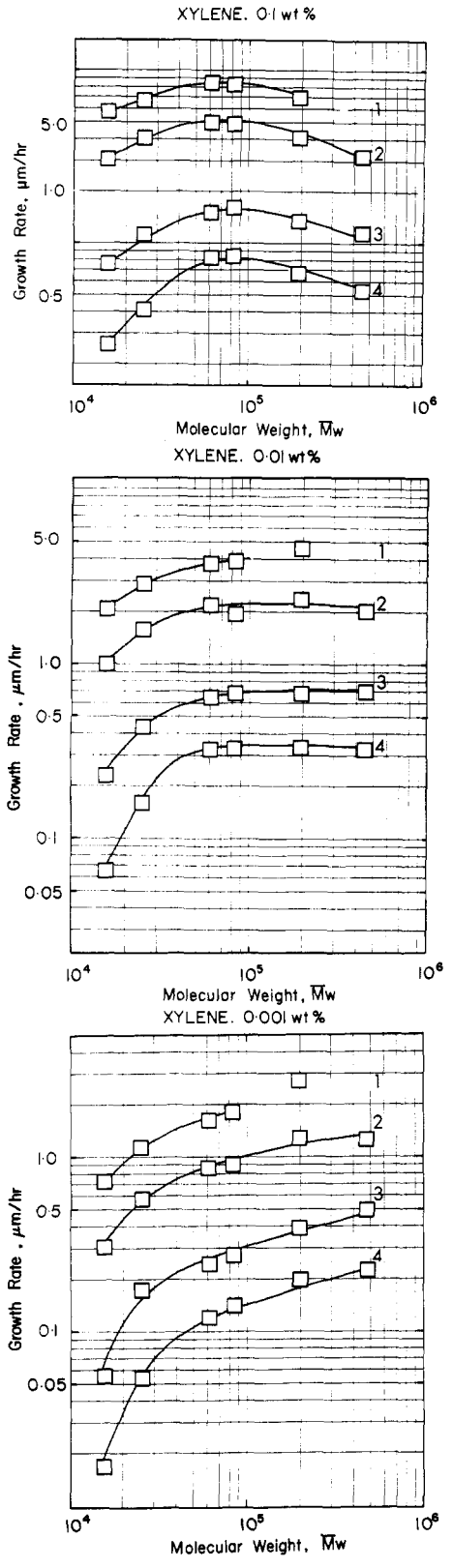

Figure 4. Variation of growth rate as a function of molecular weight for the three concentrations: top, 0.1; middle, 0.01; and bottom, 0.001 wt %. The crystallization temperatures are as follows (curve no., T_c (deg C)): 1, 86.60; 2, 87.90; 3, 89.80; 4, 90.70.

it is not possible to make a complete comparison with the results shown in Table II.

In the present work it is confirmed that the value of α increases with crystallization temperature for all but the sample of highest molecular weight (Figure 2). When comparing the values obtained for α with the different samples,

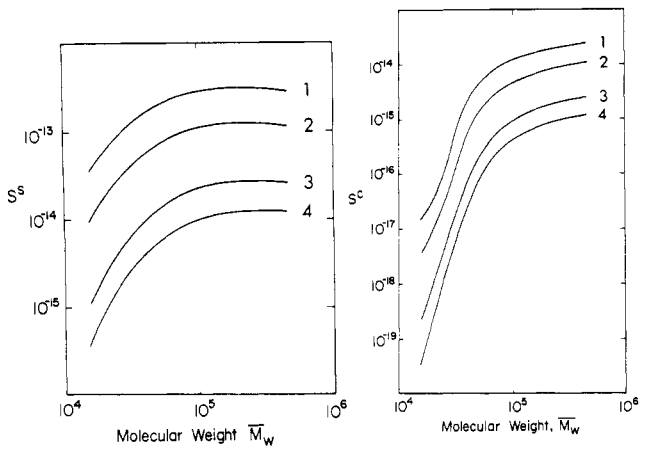

Figure 5. Left: theoretical isothermal nucleation rates for solution molecules S^s *vs.* molecular weight for 0.1 wt % concentration. Curve numbers correspond to the same temperatures as in Figure 4. Right: theoretical isothermal nucleation rates for cilia S^c *vs.* molecular weight for 0.001 wt % concentration. Curve numbers correspond to the same temperatures as in Figure 4.

it is apparent that α increases as the molecular weight decreases (Figure 3). Both findings are in accord with the predictions of the S–D theory in which it is considered that the secondary nucleation, required for continued growth of a crystal, may involve cilia as well as solution molecules.

Cilia are the dangling ends of molecules that are partially incorporated into the crystal lattice. They are formed in the following manner. The first segment of a solution molecule to deposit on a crystal growth strip would likely be not an end portion but some more central region of the molecule. When these first segments have attached to the crystal the two ends of the molecule are left dangling in solution. If now the longer end crystallizes on the growth strip by chain folding, then the other end will be left dangling as a "permanent" cilium. Sanchez and DiMarzio[6,7] proposed that these cilia could nucleate the following growth strip. Making what is considered to be a reasonable assumption, that once a new growth strip is nucleated then filling in by chain folding of molecules is a rapid process,[1-3,5] they studied theoretically the effects of molecular weight and temperature on the concentration dependence of crystal growth rates in two extreme cases.

At one extreme, cilia-nucleation was taken to be the only means of propagating the growth of the crystal (self-nucleating mechanism[6,7]), while the other extreme depends upon nucleation by molecules from solution for continued growth. When considering the specific case of polyethylene crystallized from xylene solution, it was found that in general the cilia nucleation rate (S^c) is proportional to the concentration raised to a power less than unity (fractional-order growth kinetics), whereas the nucleation rate for solution molecules (S^s) is proportional to the concentration raised to the first power (first-order kinetics) except at very low molecular weights where the concentration exponent tends to exceed unity. The concentration dependence of S^c was shown theoretically to weaken as the molecular weight is increased at a fixed crystallization temperature or as the crystallization temperature is decreased at a fixed molecular weight. The observed trends in α, as shown in Figures 2 and 3, are similar to those predicted for S^c. According to the S–D theory, α would not be expected to change noticeably from the value of 1 if polymer molecules in solution were the only source of nuclei. Accordingly some other mechanism of propagation would appear to be present. The presence of cilia nucleation can explain, at least qualitatively, the trends found by experiment.

Molecular Weight Dependence of Growth Rate. In Figure 4 the variation of growth rate as a function of molecular weight is shown at various crystallization temperatures for the three concentrations 0.1, 0.01, and 0.001 wt %.

At the concentration 0.1 wt % (Figure 4, top) the growth rate goes through a maximum as a function of molecular weight. In addition the relative positions of the points for molecular weights of 6.36×10^4 and 8.39×10^4 suggest that this maximum shifts to lower molecular weights as the crystallization temperature is lowered. The third feature is that the growth rate tails off with decreasing molecular weight more rapidly as the crystallization temperature is increased. The predicted variations of S^s and S^c were calculated as a function of molecular weight for a concentration of 0.1 wt % and at the same temperatures as were studied experimentally. Figure 5, left, shows the results for S^s. The experimental trends noted above are present in the left part of Figure 5 although the maximum which the nucleation rate goes through is broader, and the relative decrease of S^s with molecular weight as the temperature is increased is less marked in the theoretical curve. On the other hand, the theoretical curve for S^c does not go through a maximum but increases monotonically with molecular weight.

The observations noted for the experimental curves may be explained in terms of the S–D theory as follows, assuming the nucleation method of S^s to be of more importance than that of S^c at this relatively high concentration. Initially the nucleation rate (and hence the growth rate) increases with molecular weight because the undercooling ($T_d^0 - T$) is increased. This effect of increased undercooling is opposed by what Sanchez and DiMarzio refer to as a localization free energy term, the effect of which increases as the molecular weight is raised and leads to the maxima in the growth rate *vs.* molecular weight isotherms. The occurrence of this localization free energy term (F_L) is due to the energetically unfavorable approach of a molecule in solution toward the crystal. A chain molecule has to, of course, approach the crystal before any part of it can attach to the growing strip. The localization of the molecule in this fashion causes two unfavorable energy changes: the mixing entropy of polymer with solvent is reduced because of the proximity of the crystal, and the attachment of a section of the chain to the crystal face restricts the conformations available to the flexible molecule thus reducing its conformational entropy. The molecule in solution has then some tendency to oppose nucleation. This effect will increase as the size of the molecule increases and leads to the observed maximum in the growth rate on increasing the molecular weight of the polymer.

The cilia nucleation rate (S^c) and the nucleation rate for solution molecules (S^s) were calculated as a function of molecular weight for solutions of concentration 0.001 wt %. The results are shown in the right part of Figure 5 for S^c. In contrast to the S^s curves there are no maxima, S^c increasing continuously with molecular weight, as is also the case for the experimental growth rates at this concentration (Figure 4, bottom). In addition the decrease of the growth rate toward the low molecular weight end is more marked than it was at a higher concentration (Figure 4, top). The experimentally observed trends may be explained in terms of cilia nucleation, *i.e.*, we assume that S^c is the predominant means by which crystal growth is propagated at low concentration. On this basis, when considering the sharp decrease in S^c in the region of low molecular weight, we see that in addition to the nucleation rate decreasing with molecular weight because the undercooling is decreasing, the cilia, being shorter than the nominal molecular weight, would require molecules from solution to as-

sist in the stabilization of the chain-folded nucleus, hence the greater dependence of growth rate on molecular weight at low concentration. As the crystallization temperature is raised the increasing long period will result in the cilia being capable of contributing progressively fewer stem lengths to a nucleus and the participation of solution molecules then becomes more necessary, as is reflected by the increased slope of the molecular weight *vs.* growth rate curve at higher temperatures.

At the concentration 0.01 wt % (Figure 4, middle) the curve profiles lie somewhere between those exhibited at higher and lower concentration.

One may thus consider cilia nucleation to be predominant at low concentration and on increasing the concentration the effects of S^s become progressively more apparent until at 0.1 wt % the experimental curves take on the character of solution molecule nucleation.

The trends in the growth rate data under varying conditions of molecular weight, concentration, and crystallization temperature may then be explained in terms of the two methods of nucleation S^s and S^c. As shown by Sanchez and DiMarzio the total nucleation rate S will be some combination of these two terms.[7]

$$S = w_1S^c + w_2S^s \tag{2}$$

Sanchez and DiMarzio found that they could not predict values for w_1 and w_2, nor is it possible to evaluate them by using the experimental data, as will be shown below, although it was evident that w_1 is proportional to 1/mol wt since the concentration of primary cilia produced in a growth strip varies as 1/mol wt.

Relationship between Growth Rate and Nucleation Rate. For nucleation controlled growth the rate of secondary nucleation of a new growth strip is smaller than the rate at which the strip is subsequently filled in by the incorporation of polymer molecules from solution. The rate of growth of a crystal face is then proportional to the total nucleation rate S. The rate of nucleation

$$S = S^*N \tag{3}$$

(where S^* is the surface nucleation rate per nucleation site, and N the number of sites) will increase with time since the perimeter of the crystal grows larger and subsequently N increases.[6] At time t_0

$$G_0 = k_1S^*N_0 \tag{4}$$

(where G_0 is the growth rate, N_0 is the number of nucleation sites at time t_0, and k_1 is a constant), whereas at time t

$$G = G_0 \exp[kS^*(t - t_0)] \tag{5}$$

assuming S^* to be independent of time. According to eq 5, the crystal should grow exponentially with time. However, results from the present work and earlier publications[12,16,17] demonstrate that, in fact, G is independent of time. This implies that the two-dimensional growth which emanates from a nucleus must be limited to a constant length along a face. This could be due to the crystal face being uneven and growth along the edge being unable to propagate beyond steps on the surface. In this case

$$G \sim N_0S^* \tag{6}$$

where N_0 is the average number of nucleation sites between steps. We then have $S^* = S/N_0$, and G and S may be related as[6]

$$G \sim S \tag{7}$$

Using eq 2 and 7 the experimental growth rate data may be related to the corresponding theoretically calculated values for S^c and S^s by

$$G = G_s(w_1S^c + w_2S^s) \tag{8}$$

where G_s is assumed to be a constant. Values of G are available from the experimental data and corresponding theoretical values for S^c and S^s are also available. However, since the relationship between w_1 and w_2 is unknown, we have three unknowns in eq 8. This equation cannot then be used to evaluate the weighting constants w_1 and w_2.

Surface Free Energies. In the kinetic treatment of polymer crystallization the product of σ, the side surface free energy, and σ_e, the end surface free energy, is an important parameter permitting the estimation of σ_e once σ is experimentally accessible (from, for example, paraffin data[18]).

The surface free energy product has often been estimated by using the well-known relation

$$G = G_0 \exp\left[\frac{-4b\sigma\sigma_eT_d^0}{(\Delta h_f)kT(\Delta T)}\right] \tag{9}$$

where G is the growth rate (cm sec^{-1}), G_0 contains factors not strongly dependent on temperature, b is the thickness of a layer on a growing strip of a crystal (4.55×10^8 cm[19]), Δh_f is the heat of fusion (2.80×10^9 erg cm^{-3} [19]), T_d^0 is the equilibrium dissolution temperature (when considering crystallizations from the melt T_d^0 is replaced by T_m^0, the equilibrium melting temperature), and $\Delta T = T_d^0 - T$ where T is the crystallization temperature. The slope of the plot ln G *vs.* $1/T(\Delta T)$ will then equal $4b\sigma\sigma_eT_d^0/(\Delta h_f)k$ from which the $\sigma\sigma_e$ value may be calculated. A major difficulty is encountered when choosing a value for T_d^0, which is necessary to define the undercooling ΔT, and is also present in the expression for the slope.

In attempts to assess T_d^0 by experimental means, measurements have been made of the dissolution temperatures of crystals of known long periods (low-angle X-ray analysis) permitting extrapolation to infinite l. Huseby and Bair obtained a value of $T_d^0 = 113.7 \pm 1.2°$ for polyethylene in xylene by extrapolating T_d *vs.* 1/l. to 1/l. = 0.[20] Other workers used similar methods[21-24] but the results indicate that this type of experiment may not be sufficiently sensitive to evaluate T_d^0 as a function of molecular weight. It is now accepted that T_d^0 (and T_m^0) is dependent on the molecular weight of the polymer.[19,25,26]

In their analysis of the data of Holland and Lindenmeyer[16] on the growth rates of single crystals of polyethylene from dilute xylene solution, Hoffman and Lauritzen[29] used a dissolution temperature of 387.2°K (114.2°C). In that publication and in more recent reports[27,28] they demonstrated that K_g in

$$G = G_0 \exp[-K_g/T(\Delta T)] \tag{10}$$

is a function of the crystallization temperature in bulk polyethylene (see Figure 6), and that results obtained for crystallization from solution were consistent with eq 10. In bulk polyethylene above 127° (regime I crystallization, axialite morphology) $K_g(I) = 2.27 \times 10^5$ (°K),[2] while below this temperature (regime II crystallization, spherulite morphology) $K_g(II) = 1.23 \times 10^5$ (°K).[2] Using these results and the equation

$$K_g(I) = 4b\sigma\sigma_eT_m^0/(\Delta h_f)k \tag{11}$$

$\sigma\sigma_e \sim 1380$ erg^2/cm^4 (axialites), and using

$$K_g(II) = 2b\sigma\sigma_eT_m^0/(\Delta h_f)k \tag{12}$$

$\sigma\sigma_e \sim 1275$ erg^2/cm^4 (spherulites).[28] From the Holland and Lindenmeyer data for crystallization from dilute solution[16] $K_g = 2.11 \times 10^5$ (°K),[2] suggesting that the results are just on the border of regime I type crystallization. The subsequent calculation using eq 11 showed that $\sigma\sigma_e = 1280$ erg^2/cm^4.[29] This value is similar to those obtained from crystallization in the melt suggesting that a similarity must exist

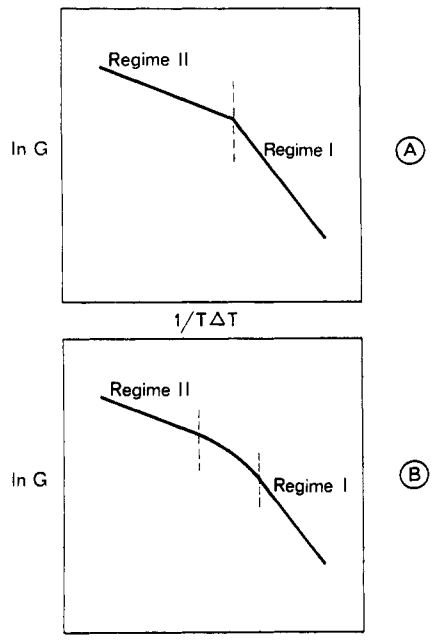

Figure 6. (A) Top: schematic representation of regime I and regime II as observed in ln G *vs.* $1/T(\Delta T)$ plot for crystallization from melt.[28] Regime I is analyzed for $\sigma\sigma_e$ using eq 11. Regime II is analyzed for $\sigma\sigma_e$ using eq 12. Note that the change in slope appears to be abrupt. (B) Bottom: schematic representation of the change over from regime I to regime II as suggested for crystallizations from solution. The intermediate region is pictured as being curved. The temperature range over which the ln G *vs.* $1/T(\Delta T)$ plot is curved may vary with molecular weight.

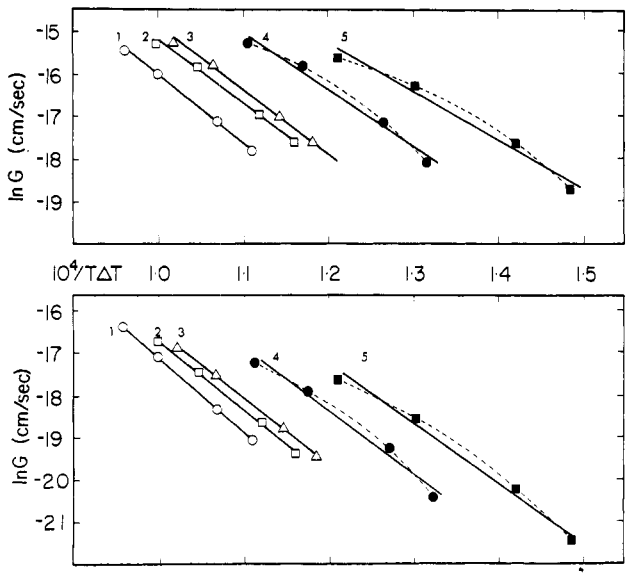

Figure 7. ln G *vs.* $1/T(\Delta T)$ plotted using Sanchez–DiMarzio values for T_d^0.[7] Curve numbers correspond to the following weights (curve no., $\bar{M}_w$): 1, 195,900; 2, 83,900; 3, 61,600; 4, 25,200; 5, 15,700. Top, 0.1 wt % concentration; bottom, 0.001 wt % concentration; 0.01 wt % concentration has been omitted but has an appearance similar to the two shown above.

in the chain-folded surface nucleus that controls the growth rate in all cases mentioned. Hoffman and Lauritzen found that a value for $\sigma\sigma_e$ of about 1300 erg^2/cm^4 leads to good agreement with the theoretical predictions for the variation of long period with undercooling in the case of melt crystallized polyethylene.[28] Because it appears that $\sigma\sigma_e$ in solution crystallized polyethylene may have a similar value, much of the discussion to follow will assume 1300 erg^2/cm^4 to be approximately correct.

Table IV
Values for $\sigma\sigma_e$ Calculated from ln G *vs.* $1/T(\Delta T)$ Plot Using Equation 11 (T_d^0 = 114.2°)

Molecular wt, $(\bar{M}_w)$	$\sigma\sigma_e$ at concn		
	0.001	0.01	0.1
15,700	1100	950	875
25,200	855	820	780
61,600	835	780	750
83,900	835	780	725
195,900	795	600	740

Table V
Values for $\sigma\sigma_e$ Calculated from ln G *vs.* $1/T(\Delta T)$ Plot Using Equation 13 (T_d^0 = 114.2°)

Molecular wt, $(\bar{M}_w)$	$\sigma\sigma_e$ at concn		
	0.001	0.01	0.1
15,700	1465	1265	1165
25,200	1140	1095	1040
61,600	1115	1040	1000
83,900	1115	1040	965
195,900	1060	800	985

Table VI
Values for $\sigma\sigma_e$ Calculated from Figure 7 Using Equation 13 (T_d^0 Values According to Equation 14)

Molecular wt, $(\bar{M}_w)$	$\sigma\sigma_e$ at concn		
	0.001	0.01	0.1
15,700	810	920	940
25,200	950	970	1040
61,600	1010	1070	1100
83,900	1080	1140	1210
195,900	1110	1200	1220

On using the value T_d^0 = 114.2° and eq 11 when analyzing the growth rate data presented in the present paper, the values shown in Table IV were obtained for $\sigma\sigma_e$ from the slopes of ln G *vs.* $1/T(\Delta T)$ curves. The values are somewhat low when compared with those discussed above. Hoffman has therefore suggested[30] that the present experimental data may correspond to the range between regime I and regime II in which case

$$K_g = 3b\sigma\sigma_e T_d^0/(\Delta h_f)k \qquad (13)$$

The results calculated using eq 13 are shown in Table V. They are closer to the values calculated by Hoffman and Lauritzen that were discussed earlier, but must be viewed with some doubt since as indicated earlier T_d^0 in fact varies with molecular weight and this has not been taken into account.

The variation of T_d^0 with molecular weight can be estimated with the aid of the following semiempirical relation suggested by Sanchez and DiMarzio[7]

$$T_d^0 = [T_m^0 - 29 + \tau_d^0]/2 \qquad (14)$$

where T_m^0 and τ_d^0 are respectively the Flory-Vrij estimates[31] for the equilibrium melting temperature and the Pennings estimates[32] for the equilibrium dissolution temperature. Using eq 14 to estimate T_d^0 for each of our polymer fractions, curves of ln G *vs.* $1/T(\Delta T)$ as shown in Figure 7 were plotted. For the present purposes it is conve-

nient to draw the best straight line through the points for each molecular weight in Figure 7 (even if the slight curvature in the data for the lower molecular weight is taken into consideration, the conclusions drawn are not significantly altered). On analysis of the slopes of these lines it was found that eq 13 gave values for $\sigma\sigma_e$ (Table VI) comparable to those values discussed earlier for crystallization from the melt. Equation 11 corresponding to regime I and eq 12 corresponding to regime II yield $\sigma\sigma_e$ values too low and too high, respectively. It thus appears that when employing the T_d^0 values calculated from eq 14 the data again correspond to the region between regime I and regime II.

A prediction of the S–D theory[7] is that if the fractional stems at the ends of the chains (lengths of chain smaller than the long period of the crystal) are rejected from the crystal they will lower the apparent surface free energy σ_e of the crystal. Since the number of such chain ends present would increase with decreasing molecular weight they suggested that the calculated value of $\sigma\sigma_e$ would increase with molecular weight. Alternatively a mode of crystal growth in which fractional stems are always incorporated would lead to defects in the crystal structure, and in this case the apparent σ_e (and hence $\sigma\sigma_e$) would tend to increase with decreasing molecular weight.

It is apparent from Table VI that the values of $\sigma\sigma_e$ increase with molecular weight, which lends support to the fractional chain rejection model for polyethylene crystals.

Let us now return to Figure 7. It is reasonable to draw straight lines through the points in the case of the high molecular weight samples. However, as the molecular weight decreases there is less certainty that the relationship remains linear. The precision corresponding to each point was sufficiently high to justify the drawing of curved lines for the lower molecular weight plots. The possible significance of the curvature will now be discussed.

Deviation from linearity in the ln G *vs.* $1/T(\Delta T)$ plots implies the following three possibilities: (a) that the product $\sigma\sigma_e$ varies with undercooling, in which case analysis of the curves in Figure 7 would require that tangents be taken to the curves at each temperature, and that the slopes of these tangents be used in eq 11, 12, or 13 to determine $\sigma\sigma_e$; (b) that the values used for T_d^0 are incorrect; (c) that the results correspond to the region between regimes I and II (hereafter to be referred to as the mid-region).

With reference to the first hypothesis, considering the small range of temperature involved, it seems unlikely that $\sigma\sigma_e$ could vary with undercooling to the extent implied by the curvature of some of the plots in Figure 7.[33] Turning to the second hypothesis it should be emphasized that the available experimental values of T_d^0 as a function of molecular weight are in good agreement with values calculated using eq 14.[19,34] Accordingly for the reasons outlined, the first and second hypotheses are assumed to be of doubtful validity. This leaves us with possibility (c). In the following section this hypothesis will be discussed and it will be demonstrated how it is compatible with the self-nucleation mechanism proposed by Sanchez and DiMarzio.

Discussion of the Observed Trends in $\sigma\sigma_e$ in Terms of the Sanchez–DiMarzio Theory (S–D) and the Hoffman–Lauritzen Theory (H–L). Hoffman and Lauritzen have demonstrated[28,29] that regime I conditions appear to pertain at low undercoolings: that is, that the filling in of a growth strip is a rapid process when compared with the rate at which such strips are nucleated. When considering the growth rate at low undercoolings one can see that since there is a large energy barrier to overcome for nucleation to occur, there will be few nuclei per unit length of strip. However, once a stable nucleus is formed the filling in of the strip proceeds rapidly. On increasing the undercooling the barrier to nucleation decreases permitting multinucleation of any given length of growth strip and the conditions predicted for regime II will be approached.

The change from regime I to regime II is not expected to be sharp but gradual as illustrated in Figure 6b. The equation governing the intermediate region would be of the form

$$K_{g\,I/II} = \frac{x b\sigma\sigma_e T_d^0}{(\Delta h_f)k} \tag{15}$$

where x will have values ranging from the value of 2, which is applicable to regime II conditions, to a value of 4, characteristic of regime I, as the undercooling decreases. If we accept the proposition that the data lie somewhere in this mid region it becomes necessary to account for the variation in curvature with molecular weight as seen in Figure 7. Each curve in Figure 7 may be thought of as a section of an overall or total regime I/regime II curve (Figure 6B). The region of the master curve from which each section derives appears to vary with molecular weight. Thus the higher molecular weight samples lie closer to the regime I end of the master curve. This implies that the number of nucleation events occurring on a given length of growth strip increases with decreasing molecular weight at any one temperature in the range studied. The presence of cilia nucleation permits the following explanation to be made concerning these observations.

Lauritzen[35] demonstrated that in regime I the rate of lamellar growth G may be expressed as

$$G = bLi \tag{16}$$

where b is the thickness of a growth layer, L is the substrate length (comparable to the distance between steps on the surface as discussed in the development of eq 6), and i is the number of nuclei per unit time per unit length of substrate (each nucleus forms a new growth layer and the average number of nuclei formed per unit time on each lamella growth face is iL). Under these conditions (*i.e.*, regime I) the velocity g, at which growth on a nucleated substrate is completed, is rapid. If g is smaller then there will be time for multiple nuclei to form on the substrate before the growth strip is completed. In this case regime II conditions apply and G then takes the form[7,35]

$$G \sim b(gi)^{1/2} \tag{17}$$

This equation will apply when L or i is very large or when g is very small. We can now look at the classification of the regimes in a slightly different way than previously and show how the S–D idea of self-nucleation becomes applicable.

Instead of considering g to be very small in regime II let us take the case in which i is large. The number of cilia formed in the most recently completed growth strip is inversely proportional to molecular weight.[7] If all these cilia have an equal probability of nucleating the next growth strip, then the greater the number per unit length, the greater the possibility that numerous stable nuclei will form. As the undercooling is increased, and hence the energetic barrier to nucleation is lowered, so multinucleation will occur more frequently. Hence, i, due to cilia nucleation, will be expected to increase as the molecular weight decreases, and for any one molecular weight i will increase with undercooling. At low undercooling all molecular weights will tend to regime I conditions (*i.e.*, one nucleation event per unit length): however, the lower the molecular weight, the smaller the undercooling at which these conditions prevail. These are the trends seen in Figure 7. The curves for the lowest molecular weight approach regime II conditions (as defined by eq 12) at high undercooling,

whereas the curve profiles tend to retain the characteristics of regime I over more of their length as the molecular weight increases.

We see then that the presence of cilia nucleation as suggested by Sanchez and DiMarzio is compatible with the regime theory of Hoffman and Lauritzen, for the existence of regimes may be due to the density of cilia per unit length of growth strip being dependent on the molecular weight. The rate at which the character of the growth changes from regime I to regime II, and the undercooling at which this occurs, appears to vary with molecular weight. However, a test of this hypothesis for dilute solution crystallization will require extension of the growth rate measurements to higher and lower undercoolings using well fractionated polymer samples. Unfortunately, using present techniques, meaningful growth rate measurements of polyethylene crystallization cannot be made outside of the range reported here. The higher molecular weight fractions could be studied at slightly smaller undercoolings, but any extension of the range of study for the remaining samples would lead to a marked loss in precision because of the very slow or very rapid growth rates involved, rendering the results of but little value.

References and Notes

(1) J. I. Lauritzen, Jr., and J. D. Hoffman, *J. Res. Nat. Bur. Stand., Sect. A*, **64**, 73 (1960).
(2) F. C. Frank and M. Tosi, *Proc. Roy. Soc., Ser. A*, **263**, 323 (1961).
(3) F. P. Price, *J. Chem. Phys.*, **35**, 1884 (1961).
(4) J. D. Hoffman, *SPE, (Soc. Plast. Eng.) Trans.*, **4**, 315 (1964).
(5) J. I. Lauritzen, Jr., and E. Passaglia, *J. Res. Nat. Bur. Stand., Sect. A*, **71**, 261 (1967).
(6) I. C. Sanchez and E. A. DiMarzio, *J. Chem. Phys.*, **55**, 893 (1971).
(7) I. C. Sanchez and E. A. DiMarzio, *Macromolecules*, **4**, 677 (1971).
(8) L. H. Tung, J. C. Moore, and G. W. Knight, *J. Appl. Polym. Sci.*, **10**, 1261 (1966).
(9) A. Peyrouset and R. Panaris, *J. Appl. Polym. Sci.*, **16**, 315 (1972).
(10) D. J. Blundell, A. Keller, and A. J. Kovacs, *J. Polym. Sci., Part B*, **4**, 481 (1966).
(11) D. J. Blundell and A. Keller, *J. Macromol. Sci., Phys.*, **2**, 301 (1968).
(12) D. J. Blundell and A. Keller, *J. Polym. Sci., Part B*, **6**, 443 (1968).
(13) T. Seto, and N. Mori, *Rep. Progr. Polym. Phys. Jap.*, **12**, 157 (1969).
(14) A. Keller and E. Pedemonte, *J. Cryst. Growth*, **18**, 11 (1973).
(15) I. C. Sanchez and E. A. DiMarzio, *J. Res. Nat. Bur. Stand., Sect. A*, **76**, 213 (1972).
(16) V. F. Holland and P. H. Lindenmeyer, *J. Polym. Sci.*, **57**, 589 (1962).
(17) M. Cooper and R. St. J. Manley, *J. Polym. Sci., Polym. Lett. Ed.*, **11**, 363 (1973).
(18) D. Turnbull and R. L. Cormia, *J. Chem. Phys.*, **34**, 820 (1961).
(19) J. J. Weeks, unpublished data as communicated to Sanchez and DiMarzio.
(20) T. W. Huseby and H. E. Bair, *J. Appl. Phys.*, **39**, 4969 (1968).
(21) J. F. Jackson and L. Mandelkern, *Macromolecules*, **1**, 546 (1968).
(22) A. Nagajima, S. Hayashi, T. Korenaga, and T. Sumida, *Kolloid-Z. Z. Polym.*, **222**, 124 (1968).
(23) T. Korenaga, F. Hamada, and A. Nakajima, *Polym. J.*, **3**, 21 (1972).
(24) E. Ergoz and L. Mandelkern, *J. Polym. Sci., Polym. Lett. Ed.*, **11**, 73 (1973).
(25) L. Mandelkern, J. G. Fatou, and C. Howard, *J. Phys. Chem.*, **68**, 3386 (1964).
(26) T. Kawai, *J. Polym. Sci., Part B*, **2**, 965 (1964).
(27) J. D. Hoffman, J. I. Lauritzen, Jr., G. S. Ross, and L. Frolen, to be published.
(28) J. D. Hoffman, G. T. Davis, and J. I. Lauritzen, Jr., "Treatise on Solid State Chemistry," Hannay, Ed., to be published.
(29) J. D. Hoffman and J. I. Lauritzen, Jr., *J. Appl. Phys.*, **44**, 4340 (1973).
(30) J. D. Hoffman, personal communication.
(31) P. J. Flory and A. Vrij, *J. Amer. Chem. Soc.*, **85**, 3548 (1963).
(32) A. J. Pennings, "Characterization of Macromolecular Structure," publication No. 1573 of the National Academy of Science, Washington, D.C., 1968, p 214.
(33) J. D. Hoffman, J. I. Lauritzen, Jr., E. Passaglia, G. S. Ross, L. J. Frolen, and J. J. Weeks, *Kolloid-Z. Z. Polym.*, **231**, 564 (1969).
(34) A. M. Rijke and L. Mandelkern, *J. Polym. Sci., Part A-2*, **8**, 225 (1970).
(35) J. I. Lauritzen, Jr., *J. Appl. Phys.*, **44**, 4353 (1973).

Thermally Induced Phase Separation Behavior of Compatible Polymer Mixtures

T. Nishi,[1] T. T. Wang, and T. K. Kwei*

Bell Laboratories, Murray Hill, New Jersey 07974. *Received October 31, 1974*

ABSTRACT: Thermally induced phase separation behavior of polystyrene–poly(vinyl methyl ether) mixtures has been studied by light transmission, optical microscope, and pulsed nmr methods. It is found that the polymer pair can phase separate by spinodal mechanism or by nucleation and growth depending upon composition and temperature. Direct proof of spinodal decomposition is provided by the nmr data which indicate a gradual change in the composition of the new phases but little change in the volumes of precipitating phases during decomposition. In addition, using the nmr data it is possible to estimate the parameters governing the kinetics of spinodal decomposition. The coefficient of diffusion is found to be negative, indicating that phase separation has taken place by the characteristic uphill diffusion. Large differences in light transmission and morphological behavior are noted during the early stages of decomposition under the two mechanisms. Most noteworthy are residual turbidity found in the sample which has apparently undergone spinodal decomposition, the high degree of interconnectivity in the spinodal structure, and the rapid rate with which such a structure is formed. The residual turbidity reaches a maximum in the PS–PVME = 20:80 mixture. By contrast, samples which have undergone phase separation by nucleation and growth exhibit no residual turbidity; the precipitating phase domains are discrete and the formation of the phase pattern is relatively slow.

In previous publications,[2] the compatibility and phase separation behavior of solvent cast polystyrene (PS)–poly(vinyl methyl ether) (PVME) films were investigated over a wide range of compositions and temperatures. The study revealed among other things the existence of a cloud point curve associated with a lower critical solution temperature.[2b,3] The result strongly suggests that there may be an unstable region within the miscibility gap where phase separation could take place by spinodal mechanism rather than by nucleation and growth.[4,5] Although the spinodal decomposition behavior has been investigated for a few polymer–solvent[6,7] and polymer–polymer[8] systems, knowledge of such phenomenon is still rather limited, especially in regard to the basic parameters which govern the spinodal decomposition process.

Earlier[2a] it has been demonstrated that the volume fractions as well as the composition of phases in the PS–PVME system can be determined with relative ease by the pulsed nmr technique. Since one of the important characteristics which differentiates the spinodal mechanism from nuclea-